RESEARCH PAPER

Development of Rectangular Vibration Isolators with Double Core Systems for Structures

Diyar Altalabani[2] · Farzad Hejazi[1]

Abstract

One of the best techniques for isolating structures from the ground is the seismic isolation technique. Nowadays, square and circular base isolators are the most frequently employed shapes. Nevertheless, these configurations are not applicable for the wall-like structures; since the applied loads are not distributed in a way that provides a uniform support condition along the shear walls. To address this issue, attempts were made to develop novel rectangular isolators with lead/rubber cores. A total of five large-scale rectangular isolators were experimentally tested and subsequently subjected to finite element analysis. A rectangular seismic isolator having double lead cores was proposed to improve its effectiveness. Exposure to lead-containing materials has been shown to have poisonous effects on both the human health and environment. To avoid this, an isolator having double rubber cores was developed. Moreover, the rubber cores are wrapped with one layer of CFRP sheet and stainless steel tube to enhance the damping ratio of the rectangular isolators. Thereafter, the novel isolators were implemented in a 10-storey tunnel-form building using nonlinear dynamic analyses. The seismic performance of the buildings was then studied by conducting Incremental Dynamic Analyses. The experimental outcomes demonstrated that confining the rubber cores by stainless steel tube and CFRP sheet increased the energy absorption along the length of the isolators by 15 and 7%, respectively. Moreover, the damping ratios of the rectangular isolator with double lead cores have also increased by 36 and 47% along its length and width, respectively.

Keywords Rectangular seismic isolators · CFRP sheets · Stainless steel tube · Lead/Rubber cores · Finite element analysis · Incremental dynamic analysis

1 Introduction

Seismic isolation systems are widely employed in high seismicity regions to protect the essential facilities of the buildings. Earthquake specialists have developed and built a variety of seismic base isolation devices [1]. Among others, rubber isolators with lead and rubber cores have been used extensively as seismic base isolators for a variety of building and bridge structures worldwide. Although the earthquake itself is uncontrollable, the real effects on the structures can be reduced by using seismic base isolators to reduce the impacts of foundation movement on the superstructure. The isolation system improves the energy dissipation capacity and stability of the structure by inserting base isolators between the foundation and the superstructure. Rectangular base isolators have seldom been examined for wall-like structural systems, despite the fact that the utilization of conventional seismic isolators may be recognized in a number of countries around the world [2–6]. The main assumption used in the design of base-isolated structures is that they will behave elastically to the seismic excitations. It is anticipated that the isolators, which are made to be easily replaceable, will sustain the majority of the damage carried on by seismic forces. Isolated structures are resilient because they were designed to be low-damage and quickly restored, which are resilience concepts. The usage of alternating steel shims with rubber layers improves the vertical rigidity to support the

✉ Farzad Hejazi
farzad.hejazi@uwe.ac.uk

1 Department of Civil Engineering, Al-Qalam University College, 36001 Kirkuk, Iraq

2 Faculty of Environment and Technology, The University of The West England, Bristol, UK

structures self-weight and the lateral flexibility of the isolators [7].

Several research studies investigated the mechanical simulation of the seismic isolators under seismic excitations [8]. conducted an experimental study on the influence of incorporating LRDs in chevron-configured special concentrically braced frames. The results revealed that the bearing having a large lead core diameter had a greatest energy dissipation capacity [9]. used sensitivity analyses to investigate the seismic performance of square lead-rubber bearings. A total of 81 bearings with various variables were tested. The diameter of the lead plug was found to be the most powerful parameter in affecting the quality of the bearings, while the volume of elastomer content had the minimum impact [7, 10]. investigated the performance of laminated rubber bearings under the effect of various axial loadings using numerical methods. According to the findings, increasing the axial compressive load resulted in a significant reduction in isolator stiffness [11]. tested the limit states of lateral stability and shear failure of seismic base isolators for a bridge using experimental outcomes. The study's results indicated that the operating conditions appeared to be nearly unachievable, and that it is not possible to identify experimentally why the majority of rubber isolator devices fail without exhibiting any damages [12]. proposed a robust analytical model capable of predicting the isolator's behaviour under cyclic shear tests with perfect accuracy. A study was performed by [13] to develop a novel seismic rubber isolator incorporating stainless steel rings with rubber core via finite element modelling. The model was called "Ring Rubber Isolator" when the lead core was replaced by a cylindrical rubber core. The findings revealed the improved energy absorption per cycle, higher damping ratio, and lower effective stiffness of the proposed seismic isolator device than a classical lead rubber isolator. Under combined tensile and compressive loads, [14] conducted a numerical analysis on the mechanical characteristics of seismic isolators having different rubber cores. The results proved that the isolators with different radially dispersed cylindrical rubber cores outperformed those with a single central rubber core. Furthermore, [15] investigated the lateral stability of isolation systems with circular and square configurations and having various cores of rubber using a numerical modelling. They discovered that increasing the size of the cores had no discernible effect on the isolator's lateral stability. The behaviour of building structures under coupled horizontal-vertical ground excitations has been improved, according to [16]. To efficiently weaken and dampen the earthquake excitations in the vertical direction, the multidirectional seismic isolation (MDSI) system was designed. The outcomes showed that the proposed seismic isolators minimized both vertical and horizontal accelerations by almost 55 and 25%, respectively. Moreover, [17] developed new rectangular isolators with various square rubber and lead cores subjected to earthquake excitations. The rubber cores have been wrapped with CFRP/steel to improve the viscous damping capacity of the developed isolators. The findings showed that the rubber cores confinement led to an improvement in the energy dissipation capacity of the devices. Recently, [18] investigated the influence of using lead rubber isolators on seismic behaviour of four-span steel box girder bridges. A parametric study was performed to study the effect of lead rubber bearings parameters on the isolated bridges. The results showed that the isolated steel bridges had about 20–30% lower seismic reaction than a non-isolated bridge.

One of the most efficient strategies to control the seismic vibrations of structures is to use the seismic base isolators to prevent the damage caused by the seismic events. However, since the anisotropic seismic base isolation systems have traditionally been developed by utilizing symmetrical shape rubber isolators, the most typical forms used for seismic isolators are square and circular configurations. While there are a few research on rectangular seismic isolators for shear wall constructions, adequate laboratory tests or numerical modelling of rectangular rubber isolators that apply to tunnel-shaped structures are not seen. For this purpose, a total of five large-scale rectangular isolators with and without lead/rubber cores are manufactured. On the other hand, research has shown that exposure to lead-containing materials is poisonous to both the environment and human health. Therefore, rubber cores were employed in place of lead cores to prevent any negative impacts that the lead material might have. Based on the literature, the rubber cores in typical base isolation devices are unconfined, which causes them to have a low damping ratio. Therefore, to enhance the viscous damping ratio and lateral shear behaviour of the isolators, the rubber cores are wrapped with one layer of CFRP and stainless steel tube. This study also takes into account a rectangular isolator without cores for comparison's sake. The performance of the five full-scale isolators under cyclic loads is also examined using finite element models.

2 Development of Proposed Rectangular Seismic Isolators

Currently, the bearings available in the market are mostly manufactured in circular or square shapes which are unapplicable for shear wall buildings. This is because the distribution of the loads is not providing uniform support conditions along the shear wall [17]. Therefore, in the present study, rectangular rubber isolators having double cores of lead and rubber are designed to use for shear wall

buildings. The double lead/rubber cores are implemented to provide the required horizontal stiffness as well as to increase the energy dissipation capacity of the isolators. Lead is widely regarded as a non-environmentally friendly metal. As a result, the double lead cores of a rectangular isolator were replaced by double rubber cores to minimize any adverse environmental effects induced by the lead substance. The rubber cores are then wrapped with CFRP/steel to boost the viscous damping capacity of the isolator devices. The design of the isolation systems is an iterative process. Therefore, various criteria need to be included such as vertical load, lateral displacement, diameters limitations of the cores for dissipating energy, and distances between isolators. For this purpose, the initial design of the proposed rectangular isolation devices is developed and its seismic performance is evaluated. The manufacturing processes of rectangular devices having double cores of rubber wrapped with CFRP layer and steel tube are depicted schematically in Fig. 1. The double lead/rubber

cores are intended to provide to increase the energy dissipation capacity and primary horizontal stiffness of the isolation devices. They also contribute to a greater vertical stiffness and provide hysteresis damping to the device as they undergo inelastic deformation. As these cores go beyond elastic deformation, the stiffness of the structure decreases. And, as a result, the structure's natural vibration period, which is inversely correlated with stiffness, increases. The lead material gives an additional rigidity to the system to more successfully withstand minor earthquake actions and wind loads. Steel shim layers are implemented within the rubber layers to offer the vertical stiffness as well as to control the horizontal displacement of the rubber layers as well. Additionally, after the lead cores yield, the rubber layers generate the secondary stiffness and provide the necessary restoring forces after the seismic excitation ends. The rectangular isolator without cores is also examined for the sake of comparison as a
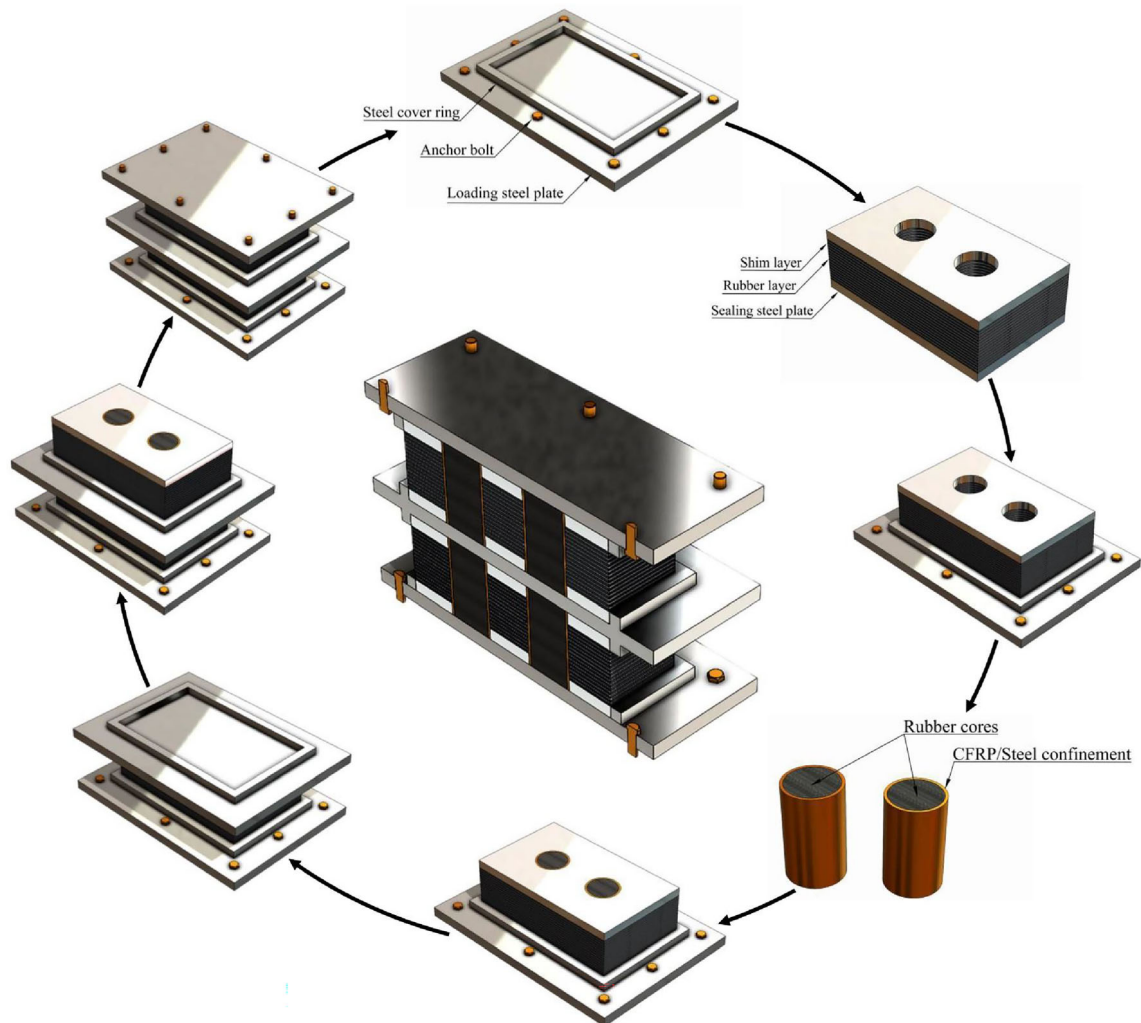
Fig. 1 Schematic illustration of the fabrication process of a rectangular seismic isolator having double CFRP/steel-confined rubber cores
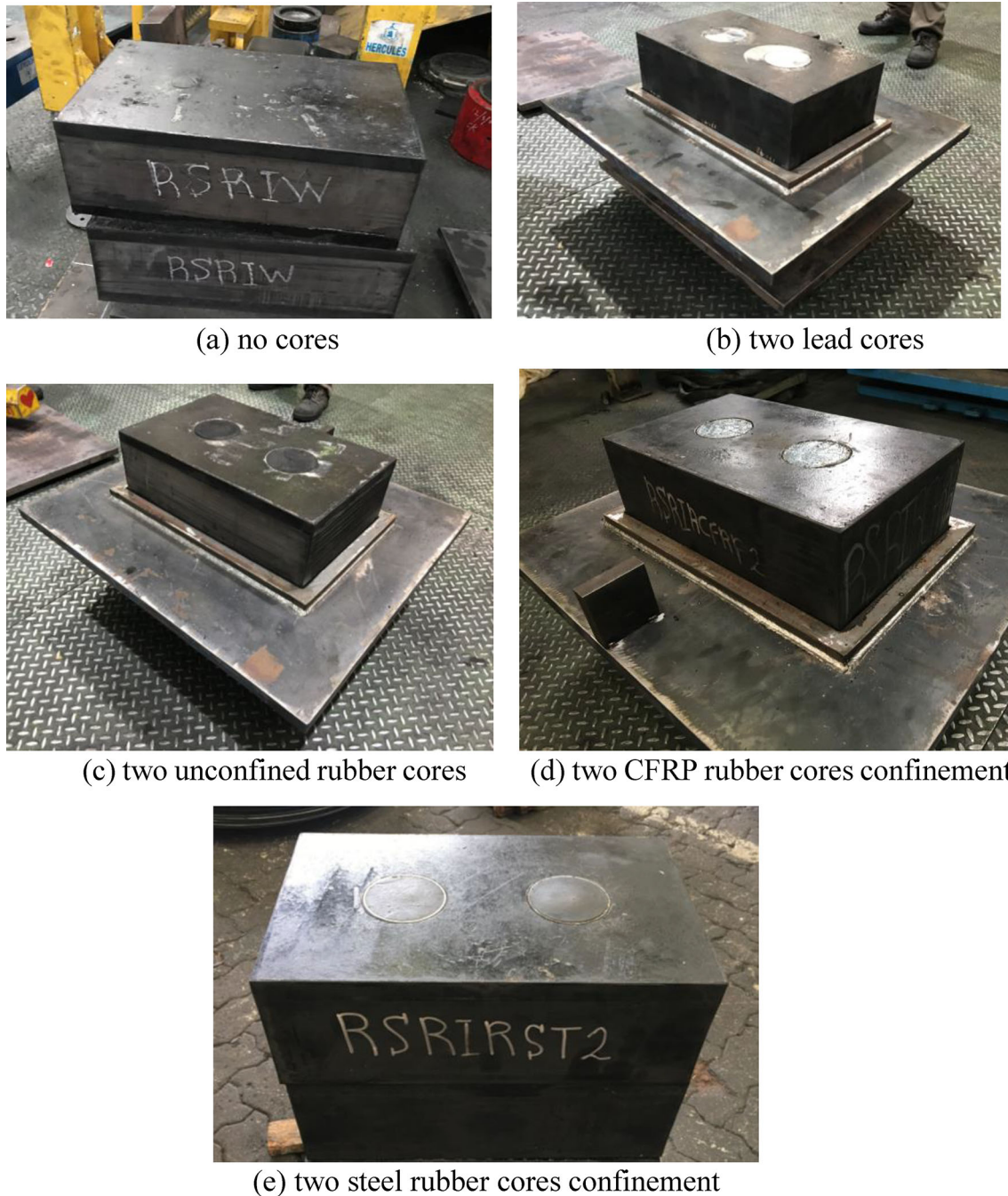
(a) no cores

(b) two lead cores

(c) two unconfined rubber cores

(d) two CFRP rubber cores confinement

(e) two steel rubber cores confinement

Fig. 2 Rectangular rubber isolators utilized in this study

benchmark. Figure 2 shows all five large-scale rectangular rubber isolators fabricated in this study.

2.1 Geometrical Properties

Figure 3 shows the typical components of the full-size rectangular isolator with double unconfined rubber and lead cores. The proposed rectangular isolators consist of three loading plates positioned at the top, bottom, and mid-

height of the bearings, four sealing steel plates, multiple shims and rubber layers, and four cores of lead and rubber. Additionally, each isolator consists of two parts (top and bottom), each part has 15 rubber layers ($n_r = 15$) and 14 steel shim layers ($n_{sh} = 14$). A covering rubber of 5 mm thickness is considered for the circumferential surface of the bearings. The rubber cores are wrapped with CFRP strip ($t_{CFRP} = 0.129$ mm) and steel tube ($t_{steel} = 3$ mm). The diameter and height of the unconfined rubber and lead
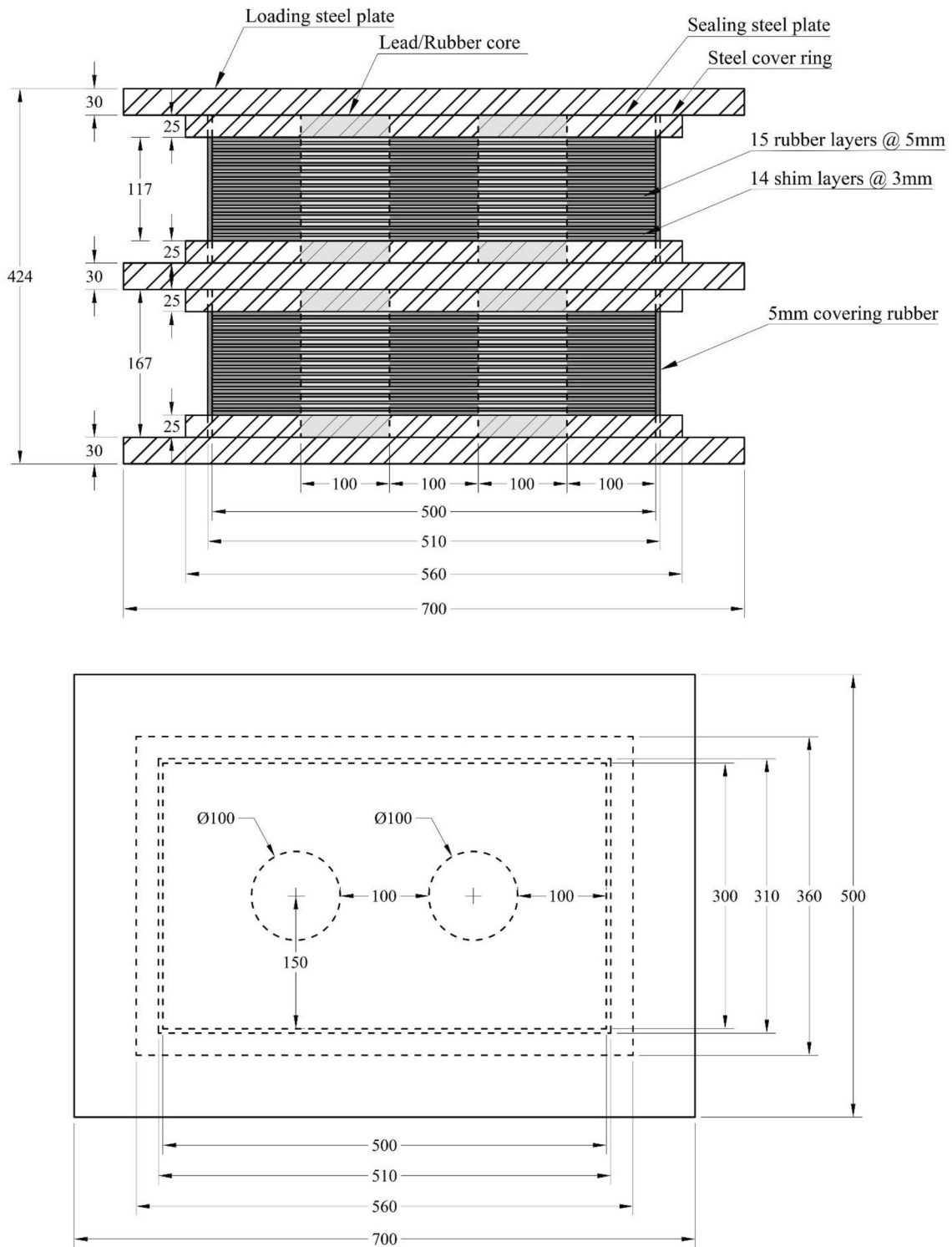
Fig. 3 Components of a large-size rectangular isolator having double lead/rubber cores. (All dimensions are in mm)

cores for each part of a rectangular isolator are $D_{\text{rubber}} = D_{\text{lead}} = 100$ mm and $H_{\text{rubber}} = H_{\text{lead}} = 167$ mm, respectively. Furthermore, the height of the isolators including the top and bottom parts is 424 mm. Table 1 shows the parameters of all models that were utilized in this research work.

Table 1 Parameters for one part of rectangular rubber isolators

Models		Description	Axial load (MPa)	Geometry details (mm)											
#	ID			$L_r \times W_r$	t_r	n_r	$L_{sh} \times W_{sh}$	t_{sh}	n_{sh}	$L_s \times W_s$	t_s	$L_1 \times W_1$	t_1		
1	RSRIW	Rectangular rubber isolator without cores	6	500×300	5	15	500×300	3	14	500×300	25	700×500	30		
2	RSRIL2	Rectangular rubber isolator with 2 lead cores	6	500×300	5	15	500×300	3	14	500×300	25	700×500	30		
3	RSRIUR2	Rectangular rubber isolator with 2 unconfined rubber cores	6	500×300	5	15	500×300	3	14	500×300	25	700×500	30		
4	RSRIRCFRP2	Rectangular rubber isolator with 2 rubber cores confined with CFRP sheet	6	500×300	5	15	500×300	3	14	500×300	25	700×500	30		
5	RSRIRST2	Rectangular rubber isolator with 2 rubber cores confined with steel tube	6	500×300	5	15	500×300	3	14	500×300	25	700×500	30		

Models		Description	Axial load (MPa)	Geometry details (mm)									
#	ID			D_{lead}	H_{lead}	A_{lead} (mm^2)	N_{lead}	D_{rubber}	H_{rubber}	A_{rubber} (mm^2)	N_{rubber}	t_{CFRP}	t_{steel}
1	RSRIW	Rectangular rubber isolator without cores	6	–	–	–	–	–	–	–	–	–	–
2	RSRIL2	Rectangular rubber isolator with 2 lead cores	6	100	167	7854	2	–	–	–	–	–	–
3	RSRIUR2	Rectangular rubber isolator with 2 unconfined rubber cores	6	–	–	–	–	100	167	7854	2	–	–
4	RSRIRCFRP2	Rectangular rubber isolator with 2 rubber cores confined with CFRP sheet	6	–	–	–	–	99.74	167	7813	2	0.129	–
5	RSRIRST2	Rectangular rubber isolator with 2 rubber cores confined with steel tube	6	–	–	–	–	94	167	6940	2	–	3

2.2 Material Properties

2.2.1 Rubber Material

The rubber-like material can be regarded as the most significant component of a seismic rubber isolator. This is because the mechanical characteristics of this material can have a direct impact on the performance of the isolation system, particularly when the base isolator is subject to lateral loading. The value of shear modulus that ranges from 0.4 to 1 MPa is considered the most significant property of the rubber material [16]. The material characteristics of the rubber are listed in Table 2. Figure 4 shows the unconfined cylindrical rubber cores.

Table 2 Mechanical properties of rubber material used in this study

Material	Hardness, IRHD[a]	Shear modulus (MPa)	Young's modulus (MPa)	Bulk modulus (MPa)	Tensile strength (MPa)	Elongation at break (%)
Rubber	60	0.4	1.35	1500	24.7	550

[a]International rubber hardness degrees

Fig. 4 Four unconfined cylindrical rubber cores

2.2.2 Lead Material

Inserting a lead material into an isolation system is meant to give the hysteresis curve an elastic perfectly plastic behaviour [8]. The stress of lead material reaches the yield point under cyclic shear force at low tension stresses of 10 MPa and demonstrates a stable hysteric behaviour due to repeated yields under cyclic load [19]. The parameters of the lead material used in this study are listed in Table 3. The cylindrical lead cores are shown in Fig. 5.

2.2.3 CFRP Material

The technical specifications of the woven unidirectional CFRP sheet with a thickness of 0.129 mm were obtained from the manufacturer's manual [20]. The ultimate tensile strength and the elastic modulus in the fibre direction are 4900 MPa and 230 GPa, respectively. The adhesive modulus of elasticity and the tensile adhesion strength are 4500 MPa and 30 MPa (7 days at + 23 °C), respectively [21]. Figure 6 shows rubber cores wrapped with one layer of a CFRP sheet.

2.2.4 Stainless Steel Material

To identify the stress–strain relationships of the stainless steel material used, a tensile coupon test was carried out. To obtain the average bending residual stresses produced due to the cold-rolling procedure, three longitudinal

Table 3 Mechanical specifications of the lead

Material	Specifications
Lead	Modulus of elasticity = 18,000 MPa
	Poisson's ratio = 0.43
	Yield stress = 10 MPa

Fig. 5 Four cylindrical lead cores

coupons were extracted at 90° from the location of the weld. To be grabbed by the test device, both ends of the coupon specimens were flattened. All three specimens were fabricated and tested according to the regulations of ASTM E8M [22]. The stress–strain diagrams of the tested coupons are displayed in Fig. 7. The cylindrical rubber specimens were inserted into the stainless steel tubes by pressure without using any types of bonds between the rubber and steel surfaces as shown in Fig. 8.

3 Experimental Program

To evaluate their performance, all rectangular seismic isolators are experimentally tested under the axial compression force and horizontal cyclic displacement. A total of five large-size rectangular isolators were fabricated and tested using hydraulic actuators with 50,000 kN vertical load capacity and 5000 kN lateral load capacity, respectively. Each rectangular isolator with both parts is set up to a double shear configuration method. Using multiple hydraulic jacks positioned at the bottom of the universal machine, the vertical compressive load is applied. Then, the lateral displacement is applied via a Programmable Logic Controller (PLC) device with a frequency of 0.04 Hz using double-action hydraulic jacks positioned on the sides of the isolator. The setup of the two parts of each rectangular isolator was to be on top of each other at the centre of the testing machine. The loading steel plates of the isolators were subjected vertically to a compression pressure of 6 MPa and horizontally to a cyclic displacement of ± 75 mm that corresponding to a 100% shear strain. According to the regulations and experimental outcomes, the maximum allowable pressure for an isolator is recommended to be (6–8) MPa [23–25]. The test was conducted at room temperature of 23 °C. Three cycles were applied to make

Fig. 6 Four cylindrical rubber cores **a** before and **b** after confinement with CFRP sheets
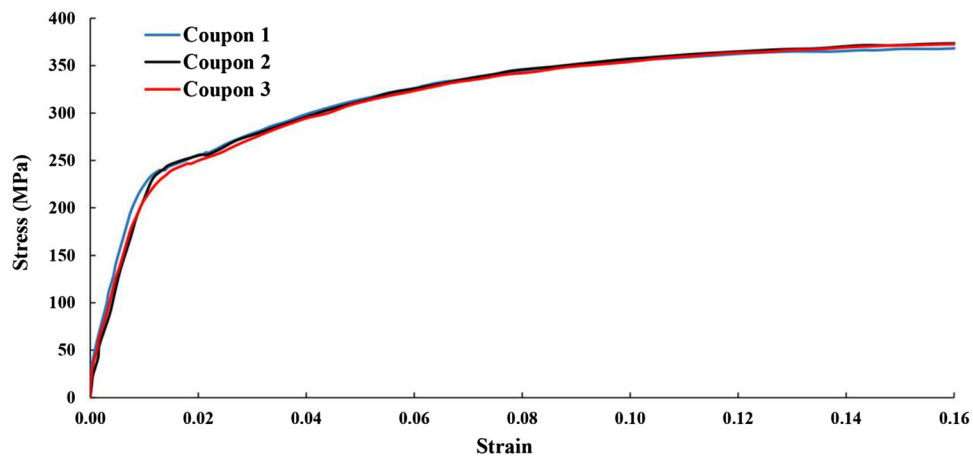

Fig. 7 Stress–strain relationships for stainless steel tube material

Fig. 8 Four rubber cores confined with stainless steel tube

Fig. 9 Overall view of the testing machine and PLC system

sure that no remarkable drop will take place in the isolator's stiffness over different repeated cycles. For the three continuous cycles, the data logger was recorded the testing

data such as pressure and displacement. The corresponding forces at each maximum and minimum value of displacements were recorded. Figure 9 shows an overall view of

(a) RSRIW

(b) RSRIL2

(c) RSRIUR2

(d) RSRIRCFRP2

(e) RSRIRST2
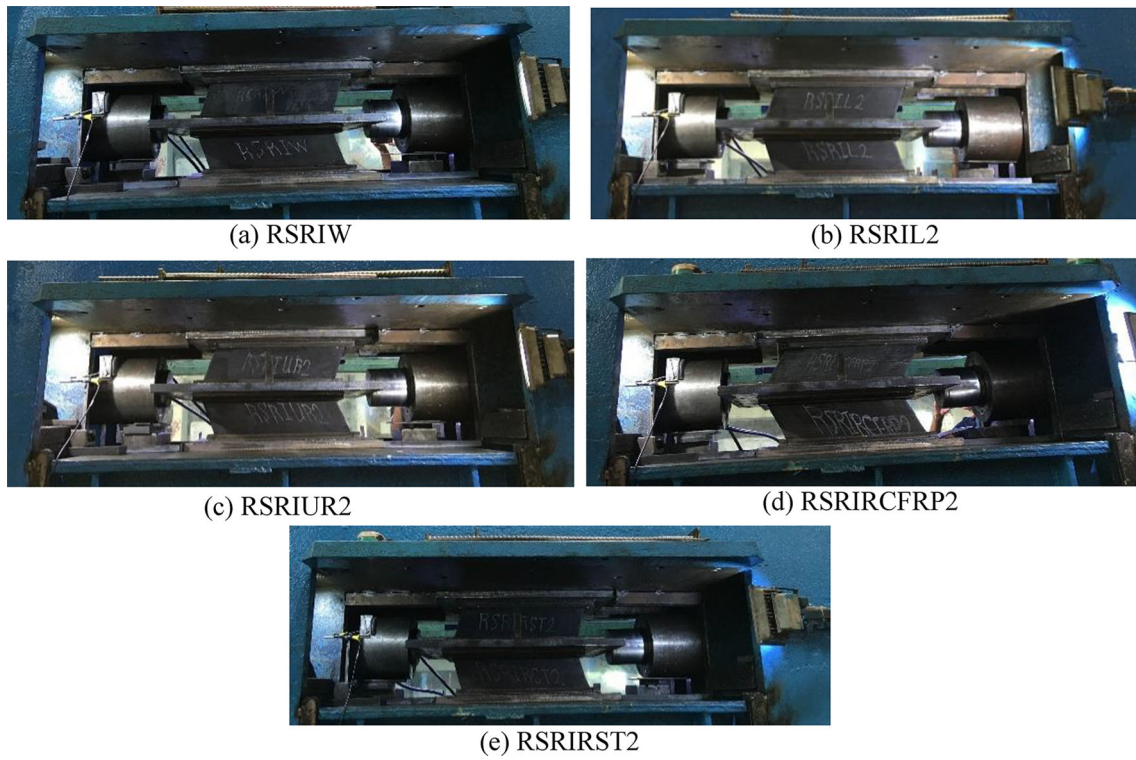
Fig. 10 Rectangular rubber isolators tested along its length

(a) RSRIW

(b) RSRIL2

(c) RSRIUR2

(d) RSRIRCFRP2

(e) RSRIRST2
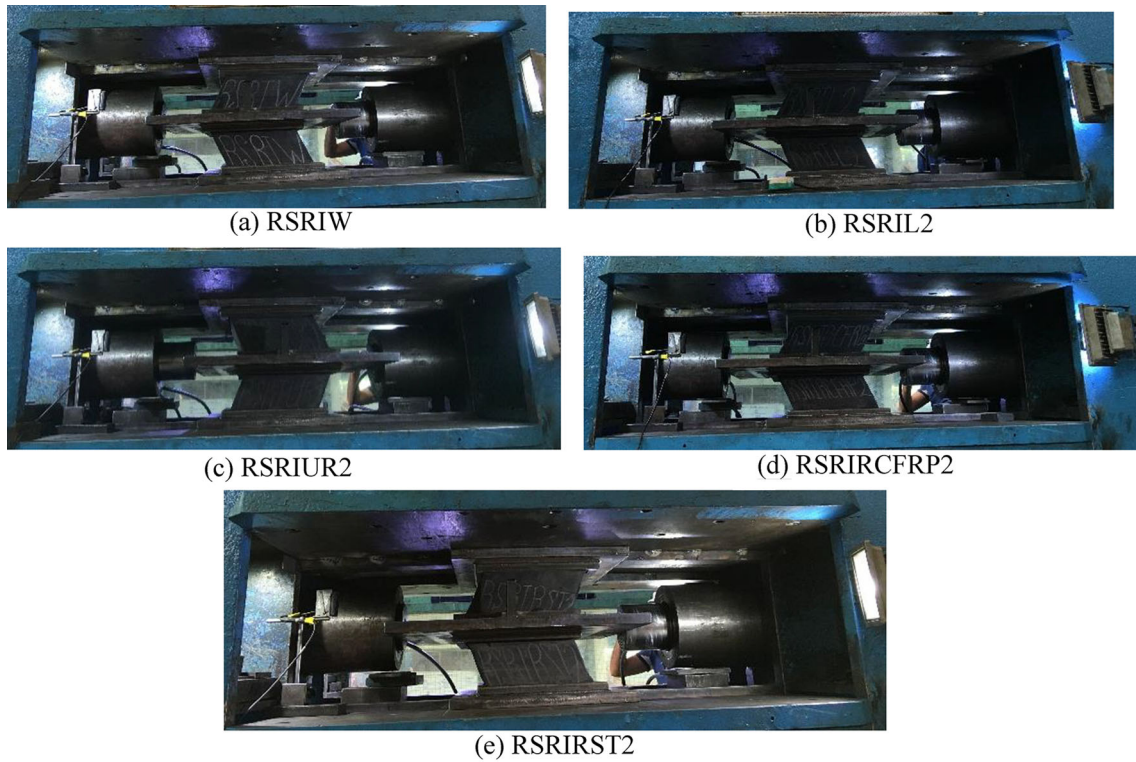
Fig. 11 Rectangular rubber isolators tested along its width

the testing machine connected to a computerized control system. Figures 10 and 11 illustrate the rectangular rubber isolators under lateral deformation along its length and width, respectively.

4 Experimental Testing Results

This section discusses the experimental testing results including the hysteric response, stiffness, and viscous damping of the developed rectangular devices in both

(a) RSRIW-Length

(b) RSRIW-Width

(c) RSRIL2-Length

(d) RSRIL2-Width

(e) RSRIUR2-Length

(f) RSRIUR2-Width
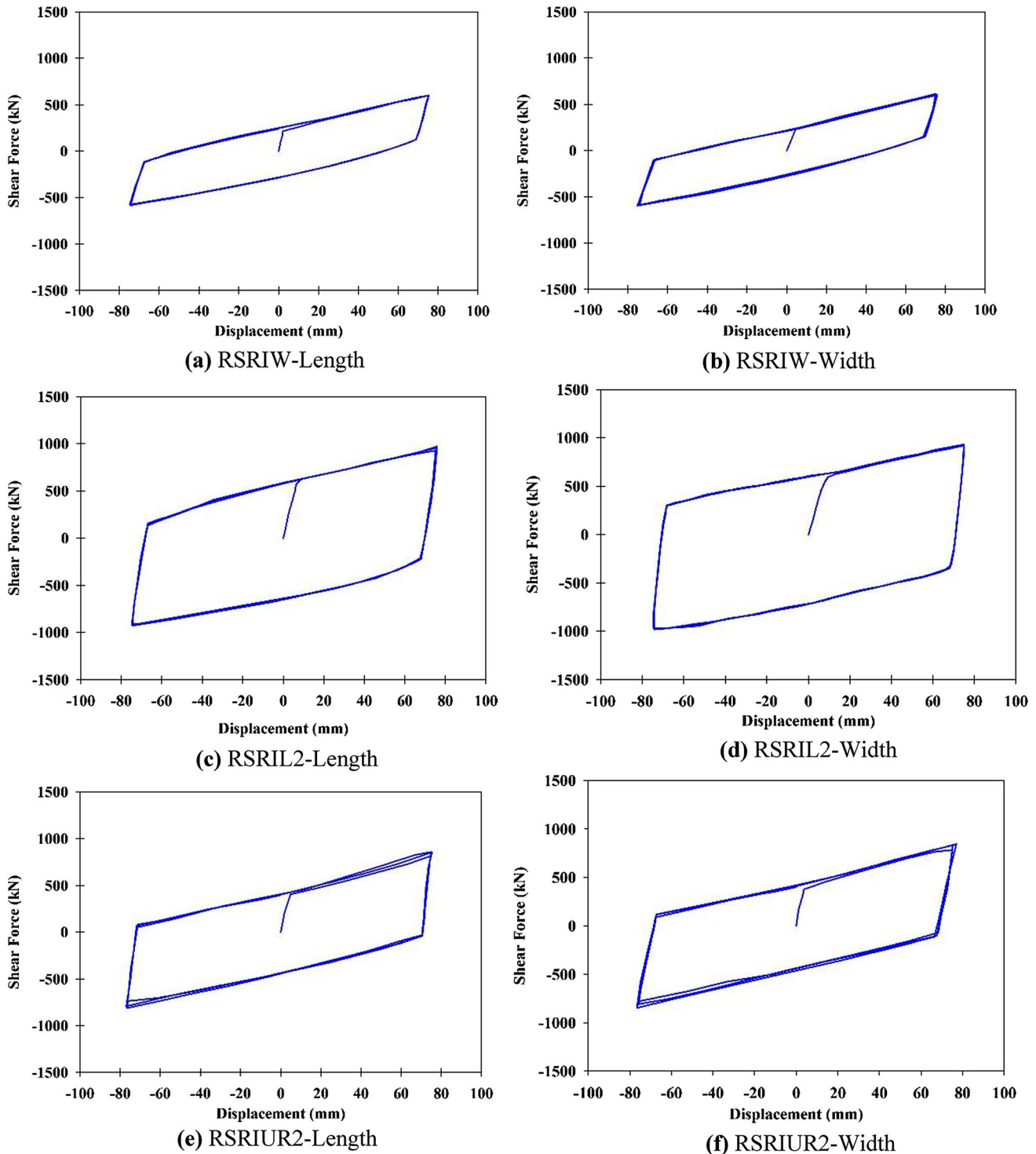
Fig. 12 Experimental results of hysteresis diagrams of rectangular rubber isolators tested along both orthogonal directions

(g) RSRIRCFRP2-Length

(h) RSRIRCFRP2-Width

(i) RSRIRST2-Length

(j) RSRIRST2-Width
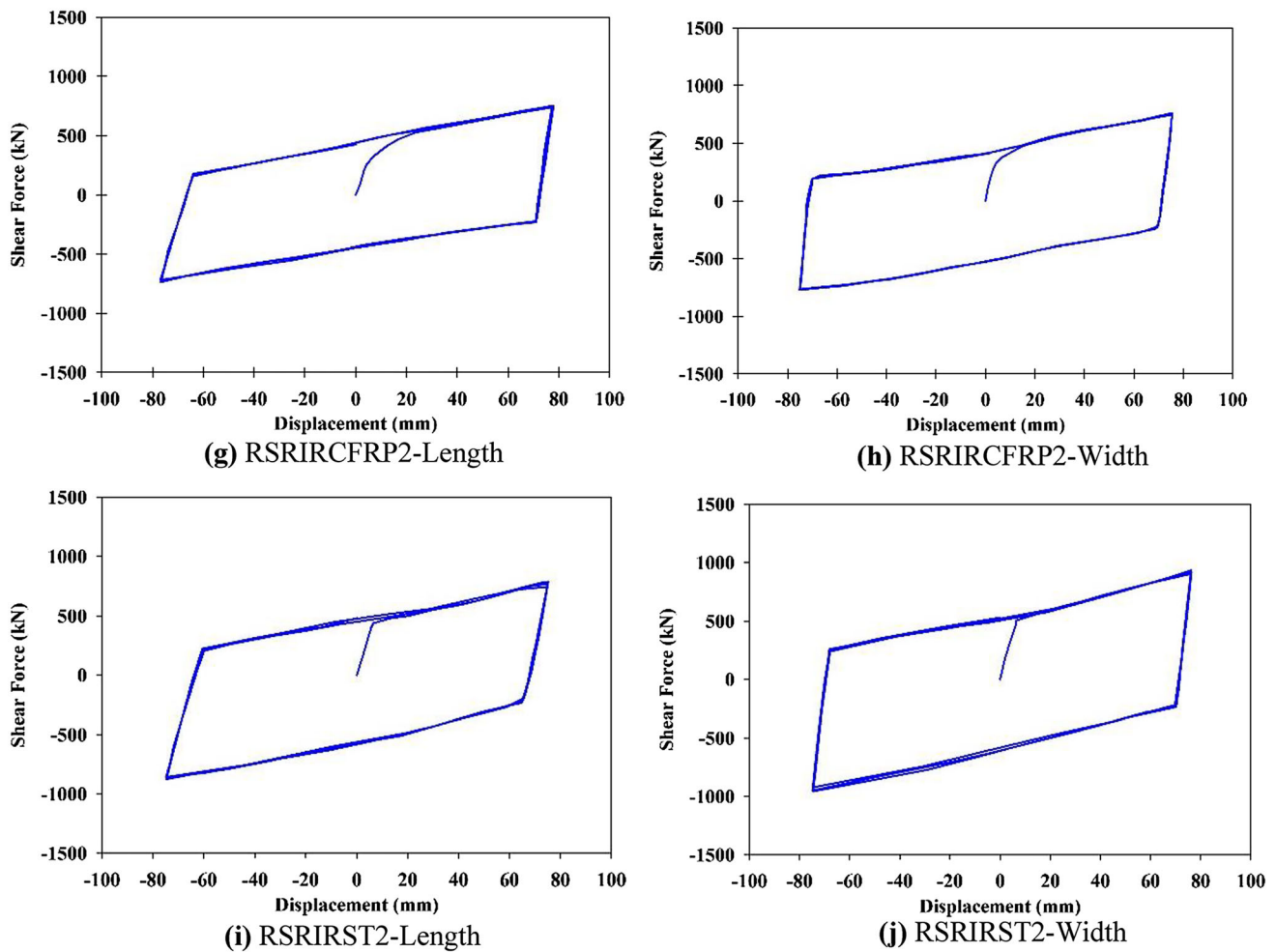
Fig. 12 continued

longitudinal and transverse directions, respectively. Figure 12 shows the results of experimental hysteretic curves for the five large-sized rectangular isolators tested along their lengths and widths, respectively. As Fig. 12 shows, all rectangular isolators exhibit a stable response along both directions. It is worth noting that isolators tested along their length show no noticeable differences as compared to those tested along their width. The horizontal stiffness of the lead and rubber cores is primarily responsible for the high stiffness of the isolators at the beginning of a cyclic shear load test. The stiffness of the rectangular isolators after the yielding of the lead/rubber cores is only because of the contribution of the rubber material, which is significantly lower than the initial stiffness. Moreover, no noteworthy variation was noticed between the forces applied in the three cycles. The damping capacity and effective stiffness of the proposed devices are calculated from the shear force vs displacement loops through Eqs. (1–4) [26]. Clearly, only small differences occurred in the hysteresis loops over the three consecutive cycles.

$$K_{h,eff} = (F_{max} - F_{min})/(\Delta_{max} - \Delta_{min}) \tag{1}$$

$$\xi = W_d/(4\pi W_s) \tag{2}$$

$$W_s = \frac{1}{2} K_{h,eff}(\Delta_{max,avg})^2 \tag{3}$$

$$\Delta_{max,avg} = \frac{1}{2}(\Delta_{max} + |\Delta_{min}|) \tag{4}$$

where F and Δ are the magnitudes of shear force and horizontal displacement, respectively. While, W_d denotes the area under the curve (dissipated energy), ξ is the viscous damping capacity, $K_{h,eff}$ is the effective horizontal stiffness, and W_s is the elastic energy.

The results of these parameters are tabulated in Table 4. The results indicate that a rectangular isolator with lead cores has the highest amount of energy dissipation of 40.01 and 42.65% along its length and width, respectively. This can be attributed to the behaviour of lead material in dissipating energy induced to the structure. Based on the results, the viscous damping ratio increases with confinement by CFRP/steel layers. For isolators having rubber

Table 4 Experimental results of rectangular rubber isolators

Rectangular rubber isolator ID	Loading direction	Displacement (mm)	Load (kN)	Effective stiffness (kN/mm)	Damping ratio ξ (%)
RSRIW	Length	75	589	7.85	29.45
	Width	75	603	8.04	29.10
RSRIL2	Length	75	942	12.56	40.01
	Width	75	952	12.69	42.65
RSRIUR2	Length	75	835	11.13	32.64
	Width	75	846	11.28	33.70
RSRIRCFRP2	Length	75	736	9.81	39.69
	Width	75	767	10.23	39.25
RSRIRST2	Length	75	823	10.97	39.11
	Width	75	946	12.61	36.71

cores, the damping ratios have increased from 32.64 and 33.70% without confinement to 39.69 and 39.25% with confinement by CFRP sheet that are tested along its length and width, respectively. It is noted that the isolator without cores has a lesser energy dissipation capacity as compared to the other isolators with cores. The reason behind this can be attributed to the damping behaviour of the elastomer layers.

5 Finite Element Modelling

The performance of the developed rectangular isolators was numerically simulated via ABAQUS package [27]. Finite element analysis was carried out in parallel with the experimental work to validate the results. The numerical investigation of the novel isolator devices is discussed in the following subsections:

5.1 Finite Element Types

The developed rectangular isolators with and without cores were modelled using solid and shell elements obtainable in the element library of the ABAQUS package [27]. In the finite element analysis software, the 3D Hex element shape was used to represent the isolators. The cylindrical lead and rubber cores, shims and rubber laminates, sealing and loading plates were all modelled using C3D8R, which has a linear eight-node solid element having three degrees of translation freedom (DOF). Furthermore, a linear four-node shell element of S4R type having six DOF at each node was used to simulate the CFRP wrap and circular steel tube, allowing for more accurate predictions. The meshed model of a developed device and its deformed shape subjected to repeated loadings is shown in Fig. 13.

5.2 Loading and Interaction

All of the surface nodes on the top and middle loading plates have been connected to two reference points (RP1 and RP2), respectively, as shown in Fig. 14. Then, the axial compressive force was applied to RP1 and lateral displacement was applied to RP2. The rectangular isolators were designed in accordance with ASCE7-16 provisions [23]. Therefore, it was determined that the horizontal design displacement of each part of the isolator is 75 mm (total thickness of rubber) that is equivalent to a 100% of rubber shear strain. The devices were subject to a ± 75-mm horizontal displacement based on the loading protocol as discussed earlier. Initially, a fixed support was considered for the bottom surface of loading steel plate and after applying the vertical load, the fixed condition was then adopted for the top loading steel plate. Translation and rotation of the top loading plate in all three directions were not allowed during the application of horizontal design displacement. The bond between the isolator parts is considered to be appropriately tied for boundary condition in the process of modelling. It is of note that this type of isolator is manufactured by applying pressure and heat to integrate the shims and rubber layers into a merged part. Therefore, these layers were fused into the mould by maintaining internal boundaries, and then, the cores of lead and rubber were incorporated into the bearings via pressure [14].

5.3 Material Modelling

The properties of materials utilized in fabricating and simulating the proposed rectangular rubber isolators are discussed as following:
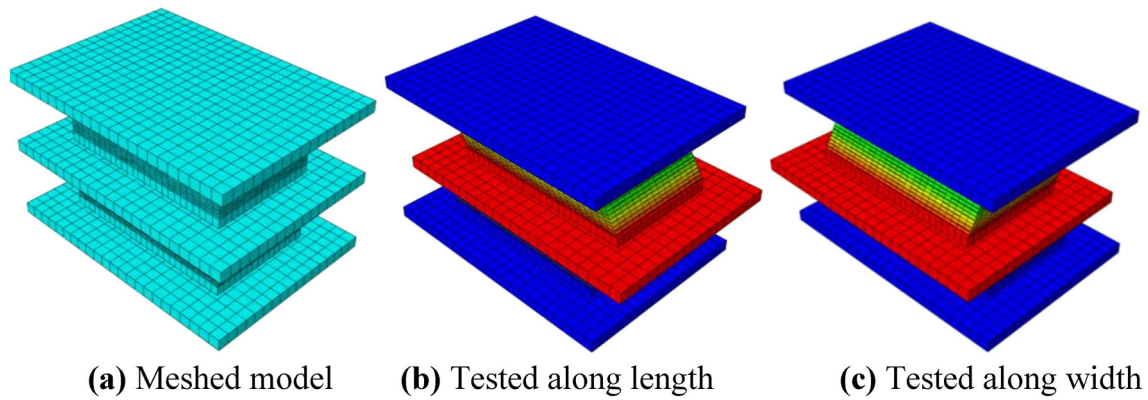
(a) Meshed model   **(b)** Tested along length   **(c)** Tested along width

Fig. 13 Rectangular isolator model and its deformed shape with mapped mesh
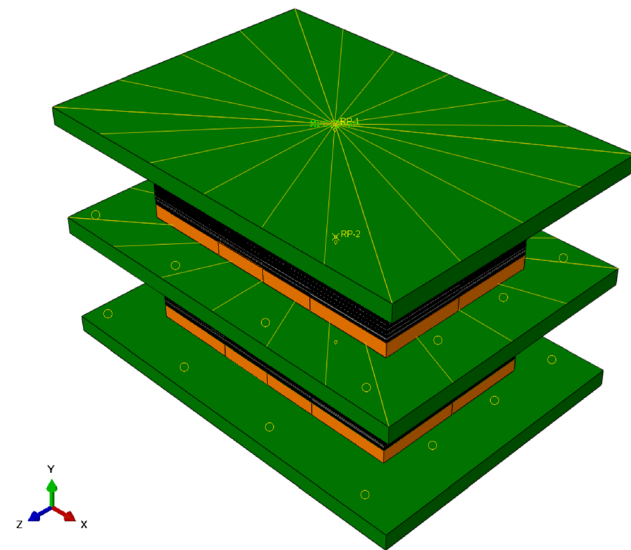

Fig. 14 Loading steel plates of a rectangular isolator with reference points

5.3.1 Rubber Material

The most crucial task in modelling the isolators is defining the materials, particularly rubber. Despite having a nearly linear relationship at small strains, the response of rubber becomes elastic and nonlinear in high strains. Due to this nonlinearity, the modulus of elasticity and shear modulus of the elastomer change as the strain increases. The shear modulus and viscous damping capacity of rubber material are influenced by the load, temperature variations, and strain history [28]. Hyperelastic materials are those that have a nonlinear stress–strain diagram and are elastic at large strains, as defined by finite element modelling; polymers like rubber are among them [27]. Isotropic, elastic, isothermal, and incompressible behaviour can be used to model such materials. The time and loading frequency have no effect on their behaviour during the test [19]. The ABAQUS software [27] has a number of

Table 5 Parameters of the Yeoh hyperelastic model utilized for the elastomer

C_{10}	C_{20}	C_{30}	D_1	D_2	D_3
0.22	0.0044	0.00013	0.0021	0.000086	−0.000018

C in MPa

hyperelastic material types, each of which defines the strain energy function differently. Because of its simplicity in describing the properties of rubber, the Yeoh hyperelastic behaviour is applied in this paper [29]. The density of strain energy for compressible laminated rubbers is expressed in Eq. (5).

$$W = \sum_{i=1}^{3} C_{i0}(I_1 - 3)^2 + \sum_{i=1}^{3} \frac{1}{D_i}(J_{\mathrm{el}} - 1)^{2i} \tag{5}$$

where W is the strain energy density, C_{i0} and D_i are constants of the elastomer, I_1 is the strain deviator's first invariant, and J_{el} is the elastic strain volume.

The constants of the rubber in this study are based on previous experimental studies reported in [30, 31], in which rubber of various hardness was also investigated. In this paper, high damping rubber having shear modulus of 0.4 MPa and viscous damping ratio of 10% is employed. Table 5 shows the parameters of the Yeoh hyperelastic model [32]. Mullin's effect [33] has been ignored for the sake of simplicity, as is customary [34]. Rubber damping behaviour is another important mechanical property. This

Table 6 Parameters of hysteresis behavior for the elastomer

Effective stress exponent	Stress scaling factor	Creep strain exponent	Creep parameter
4	1.6	0	0.56

was accomplished by imbuing the rubber material with hysteretic behaviour [35]. provided the parameters for the hysteretic response (stress exponent, stress scale factor, creep parameter, and creep strain exponent). Because the horizontal behaviour of the rectangular isolator is being evaluated in this paper, these characteristics must be included in the hysteresis curve. This means that the hysteresis diagram is formed in the shear load behaviour of the isolator by adding specific coefficients for the rubber material. The stress scaling factor affects the viscous damping ratio of the isolators and reflects the stress ratio that is being tested. The creep parameter is a definition of the rate at which effective creep strain develops. Additionally, this parameter aids in the equation's dimensional consistency. Generally, the stress exponent is greater than zero, indicating that the percentage of creep strain is dependent on effective stress. Table 6 summarizes these aspects [35]. defined the creep strain exponent as -1; this value is set to zero because the ABAQUS package does not allow negative numbers. The fact that such parameters are unitless must be noted [27].

5.3.2 Lead Material

The lead material contributes substantially to the damping behaviour of the proposed rectangular isolator having lead cores. The lead material was modelled as having elastic–plastic behaviour with properties mentioned earlier in the experimental part of this study.

5.3.3 CFRP Material

The CFRP wrap was modelled in the ABAQUS package [27] as a laminated linear elastic composite. The Hashin failure criteria was not considered because failure mode and damage behaviour are not our concerns in this work.

5.3.4 Steel Material

In this study, the bilinear elasto-plastic steel model was utilized with a modulus of elasticity $E = 205$ GPa, Poisson's ratio is $v = 0.3$, Von Mises yield criterion is $\sigma_{0.2} = 530$ MPa, and a thickness of 3 mm according to the literature [36–39]. The engineering stress–strain relationship (σ_{Eng}, ε_{Eng}) of stainless steel tube derived from tensile testing was converted into a true stress-true strain form (σ_{true}, ε_{true}) using Eqs. (6) and (7).

$$\sigma_{true} = \sigma_{Eng}(1 + \varepsilon_{Eng}) \tag{6}$$

$$\varepsilon_{true} = ln(1 + \varepsilon_{Eng}) \tag{7}$$

6 Validation of the Finite Element Modelling

An assessment of the reliability of the numerical modelling was conducted by comparing the outcomes of the experimental investigation with those of the numerical analysis in terms of the shear force-horizontal displacement loops as shown in Fig. 15. Table 7 illustrates the values of dissipated energy, effective stiffness, and damping capacity derived from the numerical analysis and the corresponding laboratory results. A good agreement in hysteresis curves between finite element analysis and experimental work was observed. The results of the damping ratio in the two model systems for all rectangular isolators exhibit some variations which are less than 13%. The modelling accuracy is acceptable based on the negligible variations between the numerical and experimental outcomes. It can be concluded that the finite element analysis can predict the performance of the rectangular isolators accurately via providing shear force-lateral deformation curves that match well with the experimental hysteresis loops.

7 Application of the Proposed Isolators

The behaviour of the 10-storey residential shear wall building utilized with and without the proposed rectangular isolators is further investigated in this study. Figure 16 shows the plan and 3D view of the studied shear wall building [40]. Thereafter, the structure was analyzed and designed through ETABS package [41] in accordance with ACI318-19 [42], and all ASCE7-16 [23] design provisions were met. The seismic isolation system of the building was consisted of 48 isolators. The horizontal behaviour of the developed isolators was obtained from the experimental work performed on rectangular isolation systems with and without cores. Moreover, PERFORM-3D [43] package was utilized to conduct a nonlinear modelling of the building according to ASCE41-17 [44] provisions.

During the dynamic analysis, the performance level of the structure is studied by considering two earthquake hazard levels: Design Basis Earthquake (DBE) and Maximum Considered Earthquake (MCE). According to ASCE41-17 [44] regulations, shear wall segments shall be considered slender if their aspect ratio H_w/L_w (height/length) is > 3 and shall be considered squat or short if their aspect ratio is < 1.5. Because most of the shear wall elements in this investigation are squat, shear failure normally governs their behaviour. Due to this, the shear strain was regarded as the deformation-controlled criterion for both the walls and spandrels. The "Shear Wall" segment from the PERFORM-3D package [43] was employed to simulate the walls and spandrels, and this element adopted nonlinear
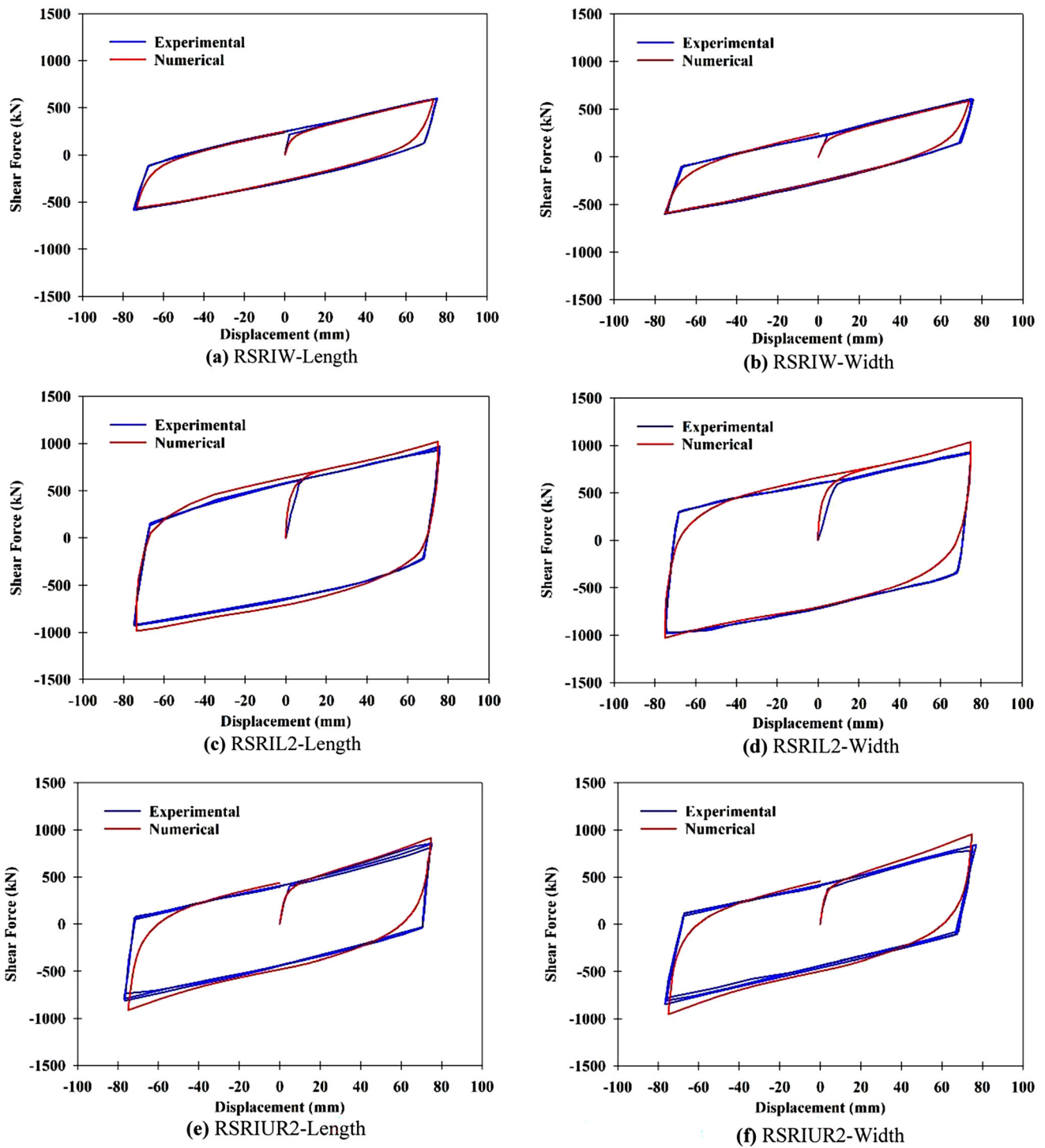
Fig. 15 Comparison of the numerical analysis and experimental hysteresis diagrams of rectangular rubber isolators tested along both orthogonal directions

shear behaviour (see Fig. 17). The global load–displacement relationships developed for the shear-controlled segments by ASCE41-17 standard [44] guided the definition of the modelling's required parameters and its acceptance criteria.

Table 8 shows the first three translational vibration periods. Accordingly, the transverse direction (y) was chosen as the major axis of the building, and the earthquake behaviour of the structure was exclusively evaluated in this direction. The fixed base structure has a first mode

(g) RSRIRCFRP2-Length

(h) RSRIRCFRP2-Width

(i) RSRIRST2-Length

(j) RSRIRST2-Width
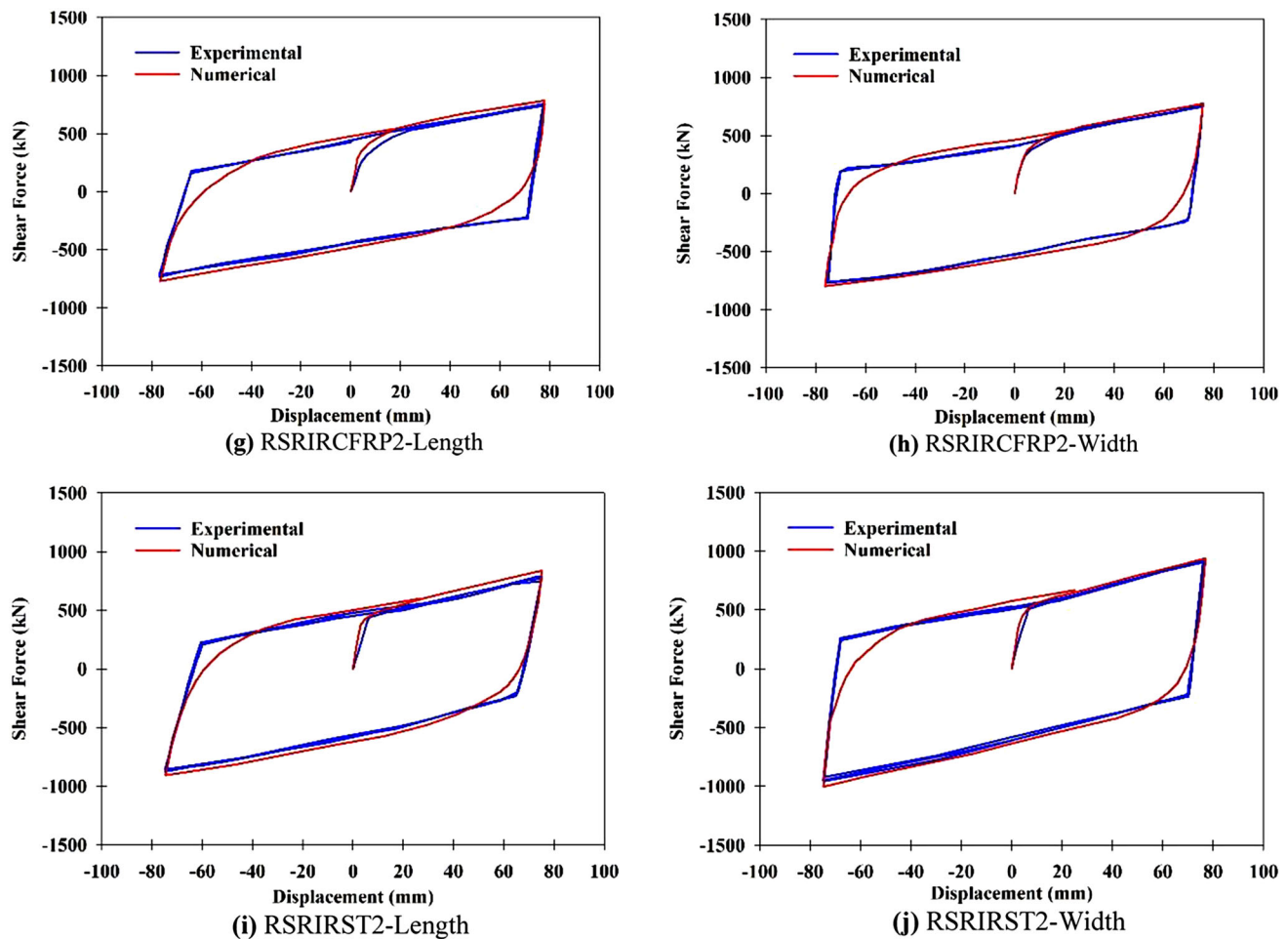
Fig. 15 continued

period of 0.248 s, whereas the base-isolated building having isolators with double lead cores has a first mode period of up to 1.3263 s. Moreover, the structure's first mode period using the developed isolators with double rubber cores wrapped with CFRP sheet increases to 1.3314 s. The results indicated that the fundamental vibration period of the isolators plays a key role in earthquake investigations on the tunnel-form buildings. This is because the seismic forces induced an excessive displacement to the structure under the increment of the vibration periods.

In accordance with ASCE41-17 [44], drift (Δ) and chord rotation (θ) were taken as the primary parameters of performance level for both the shear walls and spandrels, where the ductility was governed by the shear failure. The shear-controlled parameters are schematically represented in Fig. 18. It is noteworthy that the axial force and bending moment for the other internal forces of these elements were considered to be force-controlled characteristics. Moreover, nominal shear strength was taken into consideration, as recommended by ASCE41-17 [44], to represent the nonlinear shear response of the elements. The upper and lower bounds for the drift (Δ) and chord rotation (θ) parameters are tabulated in Table 9.

The maximum mean displacements of the mass and shear centre at each level are then described as structural responses (Figs. 19, 20). As shown in Fig. 19, the mass centre displacements for base-isolated buildings are greater than for fixed base structure, especially in the MCE hazard level. This is caused by the large displacement at the foundation level of base-isolated structures, whereas the upper stories behave more rigidly than the foundation.

It is important to note that adopting rectangular seismic isolators in base-isolated models resulted in a decrease in the storey shear force in comparison with the fixed-base model for both hazard categories, as illustrated in Fig. 20. Moreover, Interstorey Drift Ratio (IDR) for models with base isolation systems is lower than for fixed-base structures for both hazard levels. This shows that the base-isolated models' displacement and movement are uniform, and the amount of drift between the stories is minimal. For instance, for both hazard levels, the reduction in the values of the Interstorey drift ratio in the fifth storey for the

Table 7 Performance of the rectangular rubber isolator models against experimental results

Rectangular rubber isolator ID	Loading direction	Analysis type	Dissipated energy (kN.mm)	Effective stiffness (kN/mm)	Damping ratio ξ (%)	Damping error percentage (%)
RSRIW	Length	Experimental	81,717.45	7.85	29.45	3.03
		Numerical	81,969.17	7.63	30.37	
	Width	Experimental	82,697.25	8.04	29.10	3.96
		Numerical	83,662.6	7.81	30.30	
RSRIL2	Length	Experimental	177,638.5	12.56	40.01	9.58
		Numerical	209,102.62	13.37	44.25	
	Width	Experimental	191,270.1	12.69	42.65	2.58
		Numerical	212,620.22	13.74	43.78	
RSRIUR2	Length	Experimental	128,383.2	11.13	32.64	0.92
		Numerical	139,108.84	12.17	32.34	
	Width	Experimental	134,357.3	11.28	33.70	4.69
		Numerical	143,953.4	12.68	32.12	
RSRIRCFRP2	Length	Experimental	137,613.9	9.81	36.69	10.99
		Numerical	151,032.6	10.37	41.22	
	Width	Experimental	141,912.8	10.23	39.25	9.96
		Numerical	161,670.7	10.49	43.59	
RSRIRST2	Length	Experimental	151,632.7	10.97	39.11	8.51
		Numerical	175,652.6	11.63	42.75	
	Width	Experimental	163,587.1	12.61	36.71	12.39
		Numerical	191,829.7	12.95	41.90	
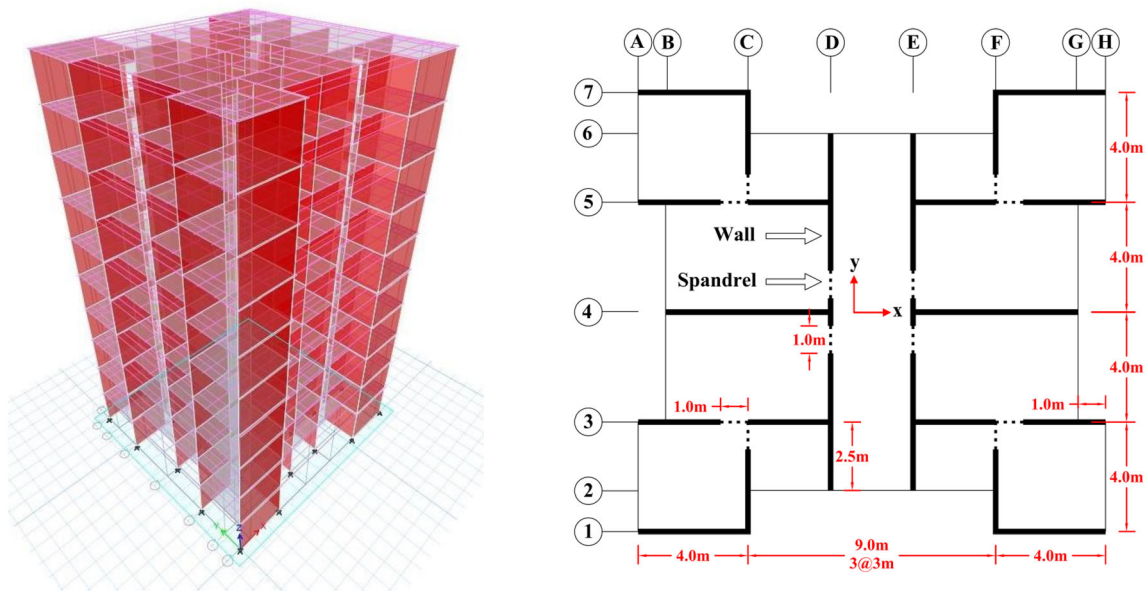
Fig. 16 Plan and 3D view of the structure [40]

RSRIRCFRP2 base-isolated model in comparison with the fixed-base model is 79 and 84%, respectively. While, the decrease in the shear force of the first floor for RSRIRCFRP2 base-isolated model as compared to the fixed base model for both hazard levels is 29 and 21%, respectively.

8 Incremental Dynamic Analysis

IDA is a computer-intensive technique that has newly been developed in many ways to conduct a detailed evaluation of building performance under seismic excitation [45]. Implementing IDA generally requires a series of steps to
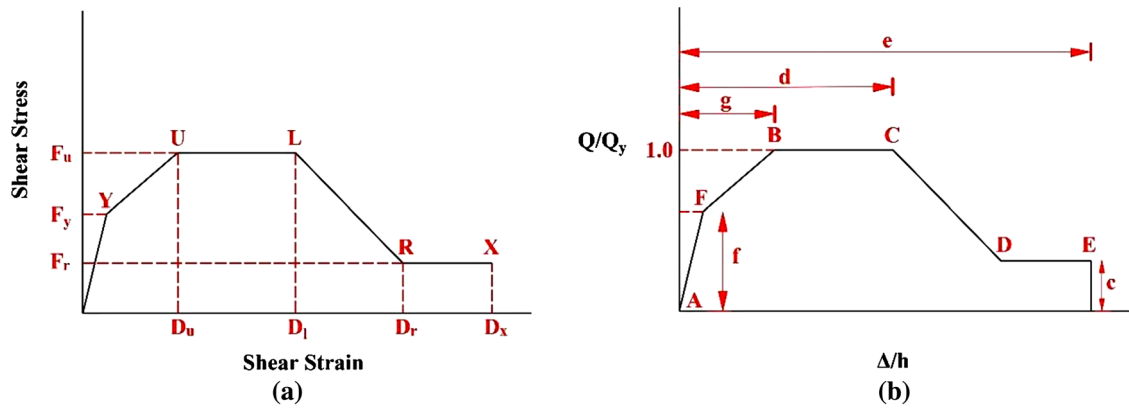
Fig. 17 The performance of nonlinear shear-control element of walls and coupling beams **a** adopted in the performance-based design software, and **b** prescribed by ASCE41-17

Table 8 The vibration period (T) and the factor of translational effective mass (M) of the studied structure

Conditions	Fixed base	RSRIW base-isolated	RSRIL2 base-isolated	RSRIUR2 base-isolated	RSRIRCFRP2 base-isolated	RSRIRST2 base-isolated
First mode (torsional)						
T_1 (sec)	0.248	1.2399	1.3263	1.3146	1.3314	1.3260
M_1 (%)	0	0	0	0	0	0
Second mode (translational along "y" direction)						
T_2 (sec)	0.176	0.8409	0.9486	0.9267	0.9483	0.9411
M_2 (%)	66.05	66.80	70.18	67.08	70.17	69.18
Third mode (translational along "x" direction)						
T_3 (sec)	0.1465	0.6429	0.7947	0.7896	0.8073	0.8022
M_3 (%)	65.99	65.75	69.43	68.59	71.41	70.61
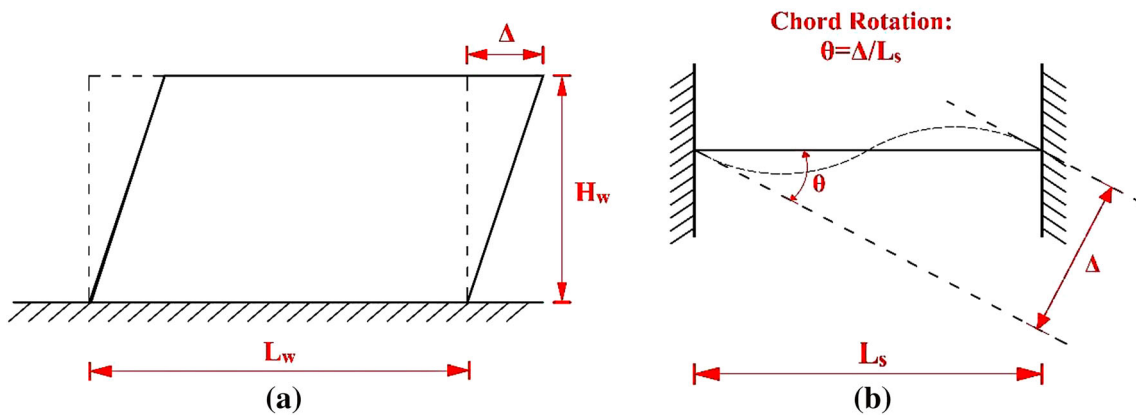
Fig. 18 The schematic illustration of the selected deformation-controlled parameters for **a** storey drift (Δ) in shear walls, and **b** chord rotation (θ) for coupling beams as proposed by ASCE41-17 when shear dominates inelastic response

Table 9 Limit states for drifts (Δ) and chord rotation (θ) (rad)

Immediate occupancy	Life safety	Collapse prevention
0.0036	0.0056	0.0075

assess a structure's seismic performance in a number of scenarios. First, a nonlinear structural model must be developed, as well as a set of recorded ground motions. After that, scale each record to various levels

(a) RSRIW base-isolated

(b) RSRIL2 base-isolated

(c) RSRIUR2 base-isolated

(d) RSRIRCFRP2 base-isolated

(e) RSRIRST2 base-isolated
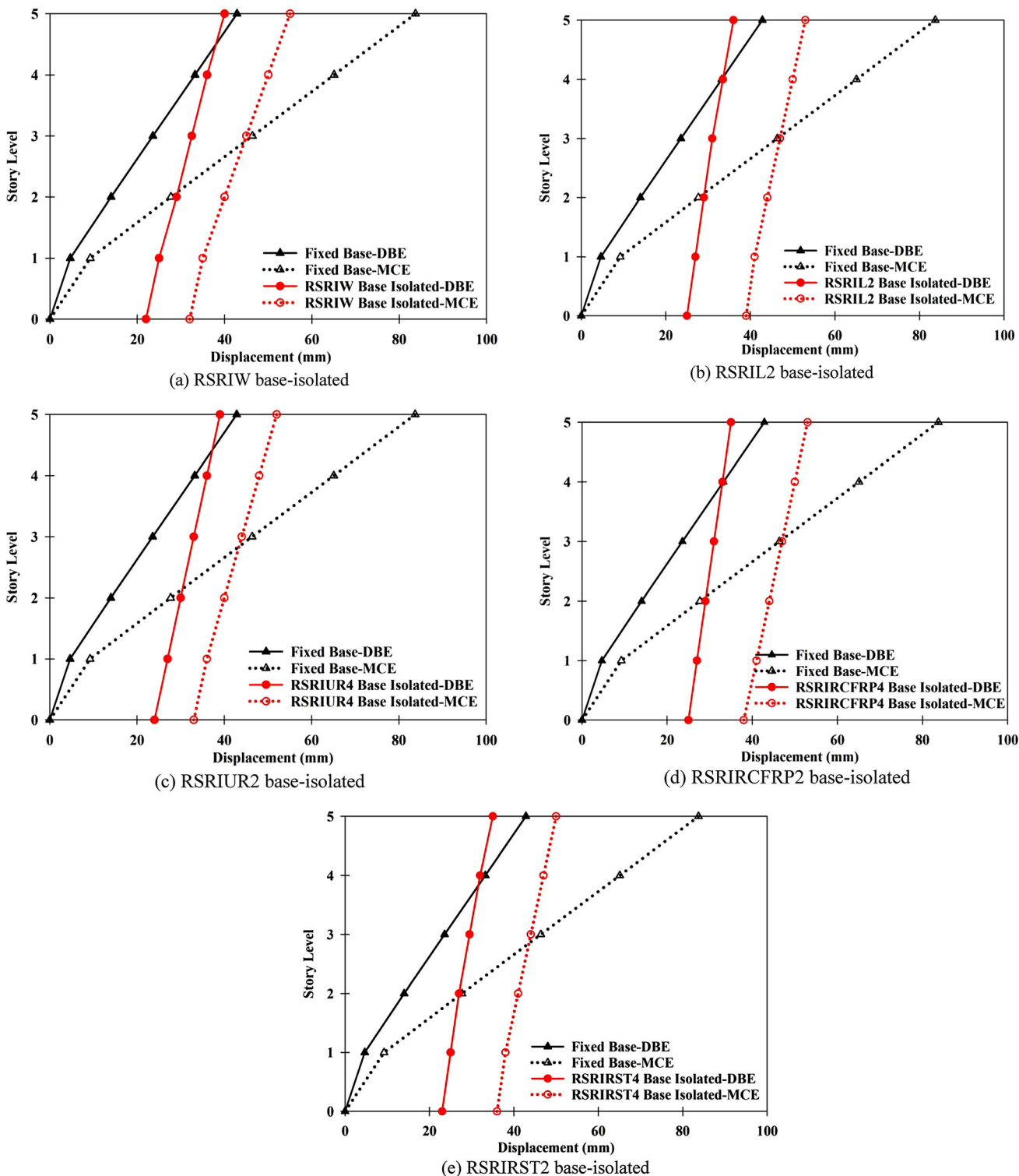
Fig. 19 Comparison of the mean values of the maximum displacement of mass centres between fixed base and various isolation systems for DBE and MCE levels

Springer

(a) RSRIW base-isolated

(b) RSRIL2 base-isolated

(c) RSRIUR2 base-isolated

(d) RSRIRCFRP2 base-isolated

(e) RSRIRST2 base-isolated
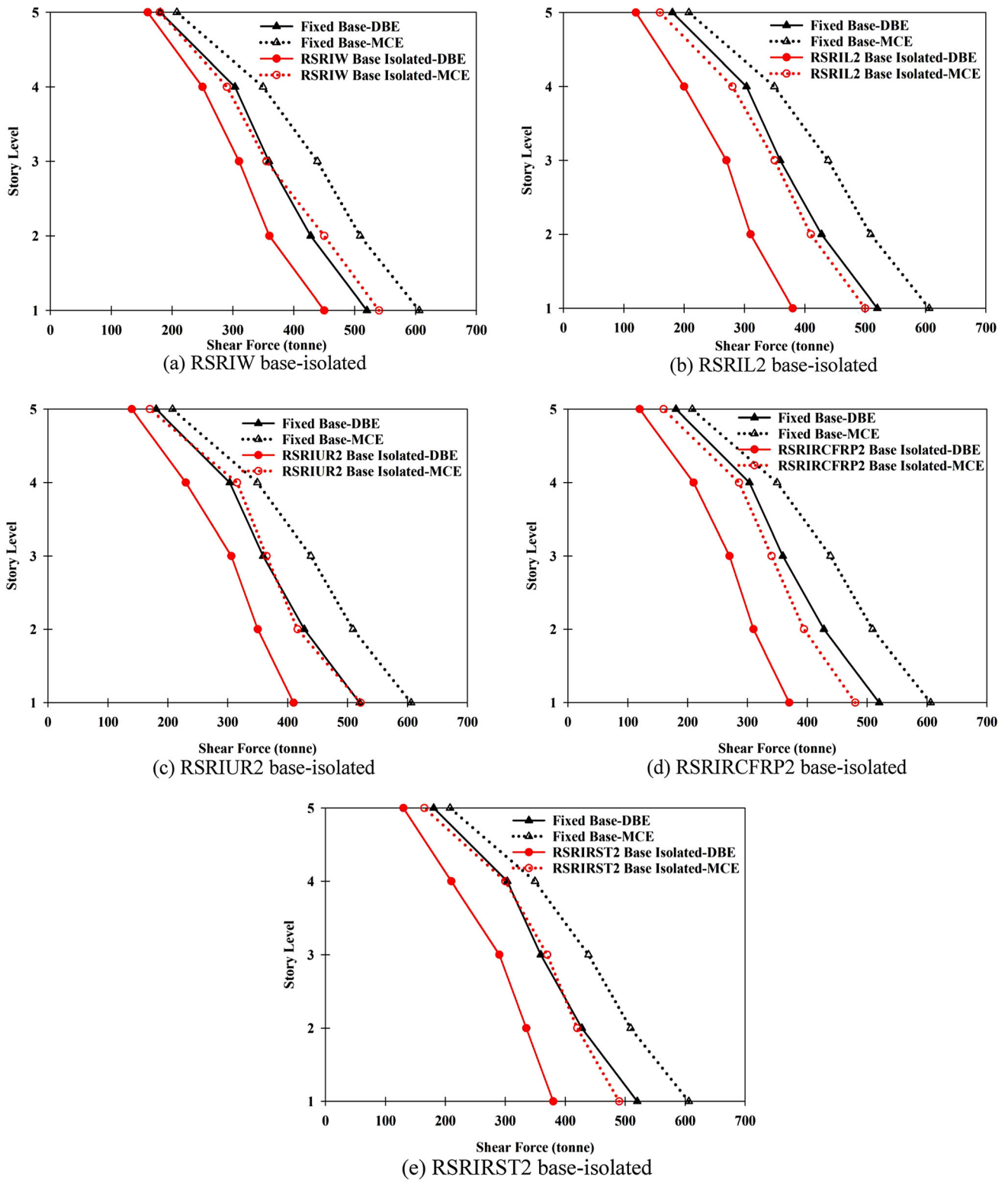
Fig. 20 Comparison of the mean values of the maximum shear forces between fixed base and various isolation systems for DBE and MCE levels

incrementally, run the nonlinear analysis, and post-process the outcomes [46]. To do so, 10 pairs of real earthquake records were extracted from the Pacific Earthquake

Engineering Research Centre (PEER) database without using any scale factor, depends on the response spectrum of the site. The details of earthquake records and acceleration
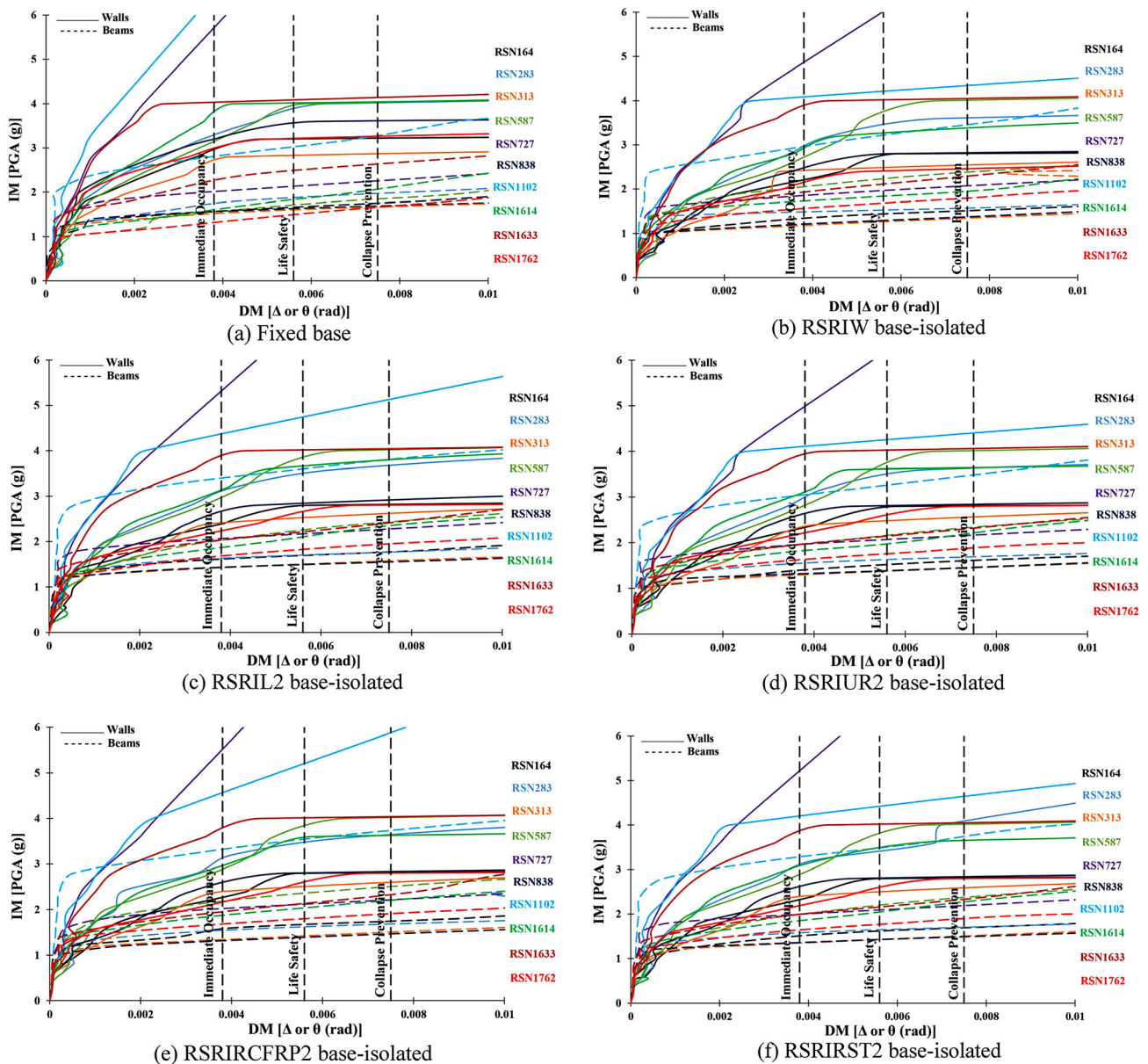
Fig. 21 Limit states and results of the incremental dynamic analyses for a structure with different rectangular isolators

response spectrum were taken from the previous research work [17]. The curves derived from the IDA are shown in Fig. 21.

Based on Fig. 21 e, f, wrapping rubber cores with CFRP/steel allowed the walls and coupling beams to exceed the different performance levels at higher PGA as compared to unconfined rubber cores. This assures the ability of these confining materials to increase the energy dissipation capacity of the isolation system. While for isolator with lead plugs, the results are almost similar to those of confined rubber cores. Therefore, there is a possibility to replace the lead cores, due to its adverse effects

on the human health and natural environment, by the confined rubber cores.

The impact of the rectangular seismic isolators on the location of damage development in the walls and spandrels was gradually investigated. The first elements indicating early failure at MCE hazard level with PGA equal to 0.8185 g were identified (red colour components) as shown in Fig. 22. A base-isolated building with RSRIRCFRP2 isolators was compared to a fixed-base building and it was observed that the damage development for a base-isolated building was considerably reduced. This brings us to the conclusion that rectangular isolators having double lead/rubber cores play a critical role in preventing shear wall
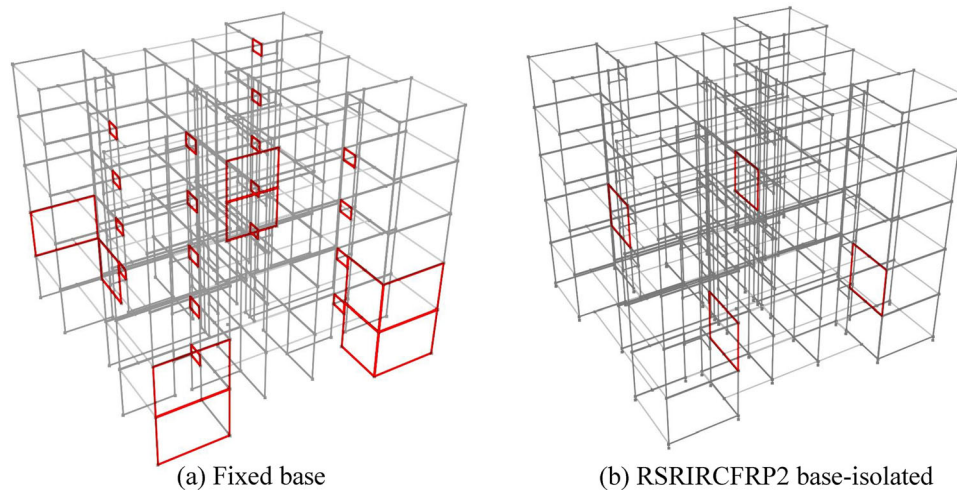
(a) Fixed base   (b) RSRIRCFRP2 base-isolated

Fig. 22 Location of first damage initiation in both the walls and spandrels for MCE hazard level

failure. In addition, the thickness of the shear walls can be reduced when using the proposed rectangular isolators and thus, the total weight of the building is significantly reduced which saves a lot of costs.

9 Practical Implementation of the Proposed Isolators

The proposed rectangular isolators are designed to implement in structures with shear wall such as tunnel-form buildings. Since this kind of building is more vulnerable against lateral loads due to its high weight to stiffness ratio, which can potentially intensify the forces induced to the structure during seismic events. To improve this vulnerability during earthquake hazards, rectangular seismic isolation systems can be incorporated into the tunnel-form structure. Most of the conventional rectangular isolators are without core systems which resulted in low damping capacity. In this study, an attempt was made to increase the

damping capacity of the rectangular isolators by using double lead and rubber cores. To achieve the desired damping capacity and energy absorption, the rubber cores were confined using one layer of CFRP sheet and stainless steel tube to increase internal friction in the material. The implementation of two rectangular rubber isolators without cores which were installed beneath each wall is depicted in Fig. 23. The lateral response of a rectangular isolator is significantly influenced by its aspect ratio (length along the loading direction to total isolator height). Testing of rectangular isolators along their length exhibited noticeable response and high damping. In practice, the rectangular isolation system could be made up through multiple rectangular isolators arranged perpendicularly or parallel in buildings with shear wall to effectively diminish vibration effect and prevent of any structural damage during applied excitation.
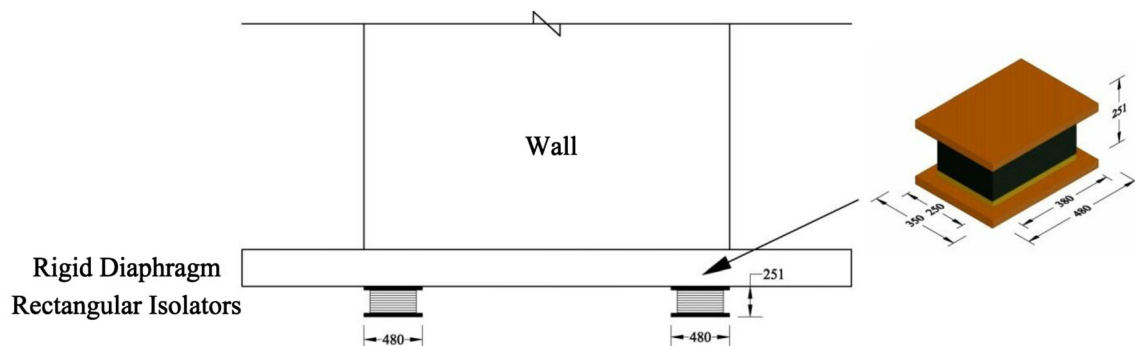

Fig. 23 Distribution of rectangular isolators under the walls

10 Summary and Conclusions

In this paper, attempts were launched to propose novel rectangular isolators with double lead and rubber cores. For this purpose, a total of five large-scale rectangular isolators were experimentally tested and subsequently subjected to numerical analysis. The experimental and numerical outcomes were then compared and showed a good agreement. Experimental hysteresis response was analyzed in both orthogonal axes under three loading cycles to ensure that no remarkable drop will take place in the hysteresis curves over repeated loadings. Moreover, incremental dynamic analysis was conducted on the fixed base and base-isolated shear wall buildings. The following are the most important findings:

(1) The findings concluded that the rubber cores confinement using CFRP/steel increased the damping capacity of the proposed devices. The energy absorbed in the rectangular isolators with rubber cores wrapped with CFRP and steel tube tested along its length is 7 and 15% greater than that absorbed by the unconfined rubber core.

(2) The damping ratios of the rectangular rubber isolator with lead cores examined along their lengths and widths have also increased by 36 and 47% as compared to that without cores. Implementing of double lead cores instead of a single core led to increase of damping capacity of the isolator due to high damping properties of the core components. As a result, the efficiency of the isolator along the direction of the wall in terms of lateral shear resistance and energy absorption capacity was remarkably enhanced.

(3) Confining the rubber cores with a single layer of CFRP and stainless steel tube led to increase internal friction between rubber particles which resulted a high damping capacity of the proposed rectangular isolators.

(4) No noticeable variations were detected between isolators that were examined along their length and those that were examined along their width.

(5) For both hazard scenarios, IDR and storey shear force for the base-isolated buildings were significantly decreased in comparison with the fixed-base building.

(6) Based on the results, confining rubber cores with CFRP/steel allowed the walls and coupling beams to exceed the different performance levels at higher PGA as compared to unconfined rubber cores.

By adopting the proposed rectangular rubber isolators, it can be concluded that the base-isolated buildings may realistically satisfy the different performance levels even under strong seismic excitations.

Data availability Data sharing is not applicable for this research study since all available data have been presented in the manuscript and there is no any further new data.

Declarations

Conflict of interest The authors have no relevant financial or non-financial interests to disclose.

References

1. Kim JH, Kim MK, Choi IK (2019) Experimental study on seismic behavior of lead-rubber bearing considering bi-directional horizontal input motions. Eng Struct 198:109529. https://doi.org/10.1016/j.engstruct.2019.109529

2. Al-Kutti WA, Islam ABM (2019) Potential design of seismic vulnerable buildings incorporating lead rubber bearing. Buildings 9(2):37. https://doi.org/10.3390/buildings9020037

3. Ismail M, Rodellar J, Ikhouane F (2010) An innovative isolation device for aseismic design. Eng Struct 32(4):1168–1183. https://doi.org/10.1016/j.engstruct.2009.12.043

4. Ounis HM, Ounis A (2013) Parameters influencing the response of a base-isolated building. Slovak J Civil Eng 21(3):31–42. https://doi.org/10.2478/sjce-2013-0014

5. Saha SK, Matsagar VA, Jain AK (2015) Reviewing dynamic analysis of base-isolated cylindrical liquid storage tanks under near-fault earthquakes. IES J Part A Civil Struct Eng 8(1):41–61. https://doi.org/10.1080/19373260.2014.979518

6. Islam AS, Al-Kutti WA (2018) Seismic response variation of multistory base-isolated buildings applying lead rubber bearings. Comput Concr Int J 21(5):495–504. https://doi.org/10.12989/cac.2018.21.5.495

7. Kalfas KN, Mitoulis SA, Katakalos K (2017) Numerical study on the response of steel-laminated elastomeric bearings subjected to variable axial loads and development of local tensile stresses. Eng Struct 134:346–357. https://doi.org/10.1016/j.engstruct.2016.12.015

8. Zeynali K, Monir HS, Mirzai NM, Hu JW (2018) Experimental and numerical investigation of lead-rubber dampers in chevron concentrically braced frames. Arch Civil Mech Eng 18(1):162–178. https://doi.org/10.1016/j.acme.2017.06.004

9. Ahmadipour M, Alam MS (2017) Sensitivity analysis on mechanical characteristics of lead-core steel-reinforced elastomeric bearings under cyclic loading. Eng Struct 140:39–50. https://doi.org/10.1016/j.engstruct.2017.02.014

10. Kalfas KN, Mitoulis SA (2017) Performance of steel-laminated rubber bearings subjected to combinations of axial loads and shear strains. Procedia Eng 199:2979–2984. https://doi.org/10.1016/j.proeng.2017.09.533

11. Gauron O, Saidou A, Busson A, Siqueira GH, Paultre P (2018) Experimental determination of the lateral stability and shear failure limit states of bridge rubber bearings. Eng Struct 174:39–48. https://doi.org/10.1016/j.engstruct.2018.07.039

12. Kumar M, Whittaker AS (2018) Cross-platform implementation, verification and validation of advanced mathematical models of elastomeric seismic isolation bearings. Eng Struct 175:926–943. https://doi.org/10.1016/j.engstruct.2018.08.047

13. Talaeitaba SB, Pourmasoud MM, Jabbari M (2019) An innovative base isolator with steel rings and a rubber core. Asian J Civil Eng 20(3):313–325. https://doi.org/10.1007/s42107-018-00107-9

14. Rahnavard R, Thomas RJ (2019) Numerical evaluation of steel-rubber isolator with single and multiple rubber cores. Eng Struct 198:109532. https://doi.org/10.1016/j.engstruct.2019.109532

15. Rahnavard R, Craveiro HD, Napolitano R (2020) Static and dynamic stability analysis of a steel-rubber isolator with rubber cores. Structures 26:441–455. https://doi.org/10.1016/j.istruc.2020.04.048

16. Pourmasoud MM, Lim JB, Hajirasouliha I, McCrum D (2020) Multi-directional base isolation system for coupled horizontal and vertical seismic excitations. J Earthq Eng. https://doi.org/10.1080/13632469.2020.1713925

17. Altalabani D, Hejazi F, Rashid RSBM, Abd Aziz FNA (2021) Development of new rectangular rubber isolators for a tunnel-form structure subjected to seismic excitations. Structures 32:1522–1542. https://doi.org/10.1016/j.istruc.2021.03.106

18. Baig MA, Ansari MI, Islam N, Umair M (2022) Effect of lead rubber bearing on seismic performance of steel box girder bridge. Mater Today. https://doi.org/10.1016/j.matpr.2022.04.953

19. Saedniya M, Talaeitaba SB (2019) Numerical modeling of elastomeric seismic isolators for determining force–displacement curve from cyclic loading. Int J Adv Struct Eng 11(3):361–376. https://doi.org/10.1007/s40091-019-00238-6

20. Sheet PD. Sika Wrap®-231 C, (2017)"Woven Unidirectional Carbon Fibre Fabric, Designed for Structural Strengthening" Applications as part of the Sika strengthening system, Version 01.01

21. Sheet PD. Sikadur®-330 2019:2–5

22. Standard ASTM (2013) E8/E8M-13a standard test methods for tension testing of metallic materials. ASTM International, West Conshohocken

23. American Society of Civil Engineers (2017) Minimum design loads and associated criteria for buildings and other structures. American Society of Civil Engineers, Reston

24. EN 1337–3 (2005) Structural bearings–Part 3: Elastomeric bearings. European Committee for Standardization, Bruxelas

25. FEMA 450–1 (2003) Recommended provisions for seismic regulation for new buildings and other structures

26. Toopchi-Nezhad H, Tait MJ, Drysdale RG (2008) Testing and modeling of square carbon fiber-reinforced elastomeric seismic isolators. Struct Control Health Monit 15(6):876–900. https://doi.org/10.1002/stc.225

27. ABAQUS®·(2014). Theory manual. Version 6.14

28. Ohsaki M, Miyamura T, Kohiyama M, Yamashita T, Yamamoto M, Nakamura N (2015) Finite-element analysis of laminated rubber bearing of building frame under seismic excitation. Earthq Eng Struct Dynam 44(11):1881–1898. https://doi.org/10.1002/eqe.2570

29. Habieb AB, Valente M, Milani G (2019) Base seismic isolation of a historical masonry church using fiber reinforced elastomeric isolators. Soil Dyn Earthq Eng 120:127–145. https://doi.org/10.1016/j.soildyn.2019.01.022

30. Shahzad M, Kamran A, Siddiqui MZ, Farhan M (2015) Mechanical characterization and FE modelling of a hyperelastic material. Mater Res 18:918–924. https://doi.org/10.1590/1516-1439.320414

31. Jerrams SJ, Kaya M, Soon KF (1998) The effects of strain rate and hardness on the material constants of nitrile rubbers. Mater Des 19(4):157–167. https://doi.org/10.1016/s0261-3069(98)00021-1

32. Habieb AB, Valente M, Milani G (2019) Effectiveness of different base isolation systems for seismic protection: numerical insights into an existing masonry bell tower. Soil Dyn Earthq Eng 125:105752. https://doi.org/10.1016/j.soildyn.2019.105752

33. Nguyen QT, Tinard V, Fond C (2015) The modelling of nonlinear rheological behaviour and Mullins effect in high damping rubber. Int J Solids Struct 75:235–246. https://doi.org/10.1016/j.ijsolstr.2015.08.017

34. Andriyana A, Loo MS, Chagnon G, Verron E, Ch'ng SY (2015) Modeling the Mullins effect in elastomers swollen by palm biodiesel. Int J Eng Sci 95:1–22. https://doi.org/10.1016/j.ijengsci.2015.06.005

35. Bergström JS, Boyce MC (1998) Constitutive modeling of the large strain time-dependent behavior of elastomers. J Mech Phys Solids 46(5):931–954. https://doi.org/10.1016/S0022-5096(97)00075-6

36. Sharif AM, Al-Mekhlafi GM, Al-Osta MA (2019) Structural performance of CFRP-strengthened concrete-filled stainless steel tubular short columns. Eng Struct 183:94–109. https://doi.org/10.1016/j.engstruct.2019.01.011

37. Hassanein MF (2010) Numerical modelling of concrete-filled lean duplex slender stainless steel tubular stub columns. J Constr Steel Res 66(8–9):1057–1068. https://doi.org/10.1016/j.jcsr.2010.03.008

38. Patel VI, Hassanein MF, Thai HT, Al Abadi H, Paton-Cole V (2017) Behaviour of axially loaded circular concrete-filled bimetallic stainless-carbon steel tubular short columns. Eng Struct 147:583–597. https://doi.org/10.1016/j.engstruct.2017.05.064

39. Hassanein MF, Kharoob OF, Liang QQ (2013) Behaviour of circular concrete-filled lean duplex stainless steel–carbon steel tubular short columns. Eng Struct 56:83–94. https://doi.org/10.1016/j.engstruct.2013.04.016

40. Mohsenian V, Nikkhoo A, Hejazi F (2019) An investigation into the effect of soil-foundation interaction on the seismic performance of tunnel-form buildings. Soil Dyn Earthq Eng 125:105747. https://doi.org/10.1016/j.soildyn.2019.105747

41. Computers and Structures Inc (CSI) (2016) Structural and earthquake engineering software, ETABS, extended three-dimensional analysis of building systems nonlinear version 16.2. 1, Berkeley

42. Committee ACI (2019) Building code requirements for structural concrete (ACI 318–19) and commentary. American Concrete Institute, Michigan

43. Computers and Structures Inc (CSI) (2016) Structural and Earthquake Engineering Software, PERFORM-3D Nonlinear Analysis and Performance Assessment for 3-D Structures, Version 6.0. 0

44. ASCE/SEI Seismic Rehabilitation Standards Committee (2017) Seismic rehabilitation of existing buildings (ASCE/SEI41-17). American Society of Civil Engineers, Reston

45. Vamvatsikos D, Cornell CA (2002) Incremental dynamic analysis. Earthq Eng Struct Dynam 31(3):491–514. https://doi.org/10.1002/eqe.141

46. Vamvatsikos D, Cornell CA (2004) Applied incremental dynamic analysis. Earthq Spectra 20(2):523–553. https://doi.org/10.1193/1.1737737